

Title: K252a prevents nigral dopaminergic cell death induced by 6-OHDA through inhibition of both MLK3/JNK3 and ASK1/JNK3 signaling pathways

Authors: Jing Pan^{*,#}, Gang Wang^{*}, Hong-Qi Yang^{*,#}, Zhen Hong^{*}, Qin Xiao^{*}, Ru-Jing Ren^{*}, Hai-Yan Zhou^{*}, Li Bai^{*}, Sheng-Di Chen^{*,#}

Affiliation: ^{*}Department of Neurology and Neuroscience Institute, Ruijin Hospital, Shanghai Jiao-Tong University School of Medicine, Shanghai 200025, P.R.China

[#]Institute of Health Science, Shanghai Institutes for Biological Sciences (SIBS), Chinese Academy of Sciences (CAS) & Shanghai Jiao-Tong University School of Medicine, Shanghai 200025, P.R.China

a) Running Title: the role of MLK3/JNK3 and ASK1/JNK3 in 6-OHDA induced dopaminergic cell death

b)Address correspondence to: Dr. Sheng-Di Chen, *Department of Neurology and Neuroscience Institute, Ruijin Hospital, Shanghai Jiao-Tong University School of Medicine, Shanghai 200025, P.R.China; #Institute of Health Science, Shanghai Institutes for Biological Sciences (SIBS), Chinese Academy of Sciences (CAS) & Shanghai Jiao-Tong University School of Medicine, Shanghai 200025, P.R.China. Tel: +86-21-6445-7249; Fax: +86-21-6445-7249; E-mail: chen_sd@medmail.com.cn

c) The number of : A) text pages:(from Introduction to Discussion): 23

B) figures: 8

C) references: 40

D) words: 1).Abstract: 242 2). Introduction: 743 3).Discussion: 1368

d) Abbreviations DA, dopaminergic; SNc, substantia nigra pars compacta; MAPK, mitogen-activated protein kinase; MAPKK, mitogen-activated protein kinase kinase; MAPKKKs, mitogen-activated protein kinase kinase kinases; ASK1 , apoptosis-inducing kinase1; JNK, c-Jun N-terminal protein kinase; MLK, mixed lineage kinase; DMSO, dimethyl sulfoxide; IP, immunoprecipitation; IB, immunoblotting; PBS, phosphate-buffered saline; TH, tyrosine hydroxylase; 6-OHDA, 6-hydroxydopaminergic; DTT, 1,4-dithiothreitol; BSA, bovine serum albumin; DAB, diaminobenzidine; MOPS, 3-(N-morpholino) propanesulfonic acid; TBST, Tris-buffered saline with 0.1% Tween 20; fluoride; SDS–PAGE, sodium dodecyl sulfate–polyacrylamide gel electrophoresis.

Abstract

It is well documented that mitogen-activated protein kinase (MAPK) pathway plays a pivotal role in rats with 6-hydroxydopamine (6-OHDA)-induced unilateral lesion in the nigrostriatal system. Our recent studies have shown that mixed-lineage kinase 3 (MLK3) and apoptosis-inducing kinase1 (ASK1) are all involved in neuronal cell death induced by ischemia, which is mediated by the MLK3/JNK3 and ASK1/JNK signaling pathway. To investigate whether these pathways are correlated with 6-OHDA-induced lesion as well, we examined the phosphorylation of MLK3, ASK1 and JNK3 in 6-OHDA rats. The results showed that both MLK3 and ASK1 could activate JNK3, and then subsequently enhance the neuronal death through its downstream pathways, i.e., nuclear and non-nuclear pathway. K252a have wide-range effects including Trk inhibition, MLK3 inhibition, and activation of PI3K and MEK signaling pathways through interactions with distinct targets and is a well-known neuroprotective compound. We found that K252a could protect dopaminergic neurons against cell program death induced by 6-OHDA lesion and the phenotypes of 6-OHDA rat model treated with K252a were partial rescued. The inhibition of K252a on the activation of MLK3/JNK3 and ASK1/JNK3 provided a link between 6-OHDA-lesion and stress-activated kinases. It suggested that both pro-apoptotic MLK3/JNK3 and ASK1/JNK3 cascade may play important role in dopaminergic neuronal death in 6-OHDA insult. Thus, the JNK3 signaling may eventually emerge as a prime target for novel therapeutic approaches to treatment of Parkinson disease, and K252a may serve as a potential and important neuroprotectant in therapeutic

MOL#38463

aspect in Parkinson disease.

Introduction

Although the expression of a number of cell death regulatory genes and receptors have been investigated in the 6-OHDA lesion model, the exact molecular mechanisms of programmed cell death underlying neurodegeneration remain poorly understood. The aim of recent studies has been set to identify the key components of the cell death machinery in dopaminergic neurons and to understand how the programmed cell death is regulated by intracellular signaling pathways.

The key components of the neuronal death machinery include mitogen-activated protein kinase kinase kinase (MAPKKK), such as mixed-lineage kinase 3 (MLK3) or apoptosis signal-regulated kinase1 (ASK1), mitogen-activated protein kinase kinase (MAPKK), c-Jun N-terminal protein kinases (JNKs) and its downstream substrates (Irving and Bamford, 2002). Among them JNK is thought to be an important kinase mediating neuronal cell death induced by 6-OHDA toxin. JNKs are members of the mitogen-activated protein kinase (MAPK) pathway that is activated in response to many extracellular stimuli and different forms of environmental stress. JNK participates in intracellular signaling pathways mediating transmission of signals from the plasma membrane to the nucleus, and is critically involved in the apoptosis following 6-OHDA injury *in vitro* (Jiang et al., 2004; Ouyang and Shen, 2006; Wilhelm et al., 2007). JNK1 and JNK2 have a broad tissue distribution, whereas JNK3 seems to be primarily localized in neuronal tissues and the cardiac myocytes (Mohit et al., 1995). Recently, MLK3, an intracellular serine/threonine kinase, has been identified as a novel upstream activator of the JNK pathway (Gallo et

al., 2002; Zhang and Zhang, 2005). At the same time, ASK1 is also considered to play a critical role in dopamine-induced apoptosis through activation JNK *in vitro* (Jiang et al., 2004; Ouyang and Shen, 2006; Wilhelm et al., 2007). Both of them function as a MAPKKK of the JNK stress pathway by directly phosphorylating and activating the JNK activators such as stress-activated protein kinase/Erk kinase-1/MAPK kinase 4 (SEK1/MKK4) and MAPK kinase 7 (MKK7). Our and other studies indicate that MLK3 and ASK1 have received attention as an important mediator of JNK-mediated apoptosis (Gallo et al., 2002; Zhang and Zhang, 2005). Thus, there may be a possibility that both MLK3 and ASK1 can facilitate dopaminergic neuron death through JNK3 activation in 6-OHDA lesion. However, whether activation of MLK3/JNK3 or ASK1/JNK3 cascade really occurs in the 6-OHDA-lesioned rats remains unknown.

Our and other previous studies on neuronal cell death induced by global ischemia focused on two possible pathways (Pan et al., 2005; Pei et al., 2006). We demonstrated that activated JNK translocates into the nucleus and phosphorylates the transcription factor c-Jun, leading to increased AP-1 transcription activity and cell death. Furthermore the activation of JNK may enhance FasL expression via c-Jun/AP-1 mediated transcriptional regulation, which can contribute to Fas receptor-mediated death. On the other hand, partially activated JNK staying in the cytosol promotes the activation of pro-apoptotic Bcl-2 family members and enhances mitochondria-mediated ischemic cell death by inducing the release of cytochrome *c* (Plesnila et al., 2001). Recently studies have linked 6-OHDA lesion with

mitochondrion-linked apoptosis signaling pathways including caspase-3 and caspase-8 (Eminel et al., 2004; Hanrott et al., 2006). But it is still unclear whether 6-OHDA-induced dopaminergic cell death is mediated by nuclear or non-nuclear pathways which occur in the above ischemic injury. Indeed, our results demonstrated that 6-OHDA-induced activation of JNK3 enhanced cell death through both nuclear and non-nuclear pathway.

K252a is originally known as a potent inhibitor of Trk, but K-252a analogs, 3,9-bis[(alkoxy)methyl] and 3,9-bis[(alkylthio)methyl]-K252a were reported as potent, selective survival-promoting agents through inhibition MLKs activation (Kaneko et al., 1997). Furthermore, numerous studies have shown that K252a has become widely used for activation of PI3K and MEK signaling pathways through interactions with distinct targets besides inhibition Trk signaling and MLKs activation. (Tischler, et al., 1991). In our previous study, we demonstrated that K252a could protect pyramidal neurons in the hippocampal CA1 region by inhibiting the activation of MLK3/MKK7/JNK3 cascade during ischemia (Pan et al., 2005). On the other hand, We also demonstrated that ASK1/JNK3 activation can be inhibited via PI3K/Akt1 pathway (Wang et al., 2007) consist with PI3K/Akt1 activation promotes cell survival by phosphorylating several substrates, including ASK1 (Brunet et al., 1999; Ozes et al., 1999). Therefore, in the present study, we evaluated K252a for protective effects against 6-OHDA injury by inhibiting both MLK3/JNK3 and ASK1/JNK3 activation. Here we demonstrated that K252a could suppress the activation of the MLK3/JNK3 and ASK1/JNK3 cascade. Furthermore, K252a could decrease 6-OHDA

MOL#38463

toxin-induced injury to dopaminergic cell bodies and terminals via nuclear and non-nuclear pathways of JNK.

Material and methods

Animals

Adult Sprague–Dawley female rats (10–12 weeks old; weighing 200–300 g at the beginning of the experiment) were used in this randomized blinded animal model study. Animals were housed in cages (n=5/cage) in the animal house under hygienic conditions in a temperature-controlled room ($22\pm 2^{\circ}\text{C}$), air quality (40–70%) and light cycle (12:12 h light:dark), and ad libitum access to standard rat chow and drinking water. Behavioral experiments were conducted between 7:00 and 13:00 h. All animals were monitored regularly and treated humanely. Adequate clean bedding and environmental enrichments were supplied.

Surgery

Rats weighing 250–300 g were anaesthetized with i.p. butaylone. When the animal was deeply anaesthetized it was placed in a stereotactic apparatus. The rats were placed in the frame, to prevent head movement, using a 45° non-puncture ear bar with the nose position 2.3 mm below the interaural line. A 2 cm incision was made and the area carefully cleared to expose bregma. A small burr hole was made with a dental drill according to the corresponding stereotactic anterior and posterior coordinates using the atlas of Paxinos and Watson (Paxino G., and Watson C 1982) to expose the dura. Rats were unilaterally injected with 6-OHDA ($4\mu\text{g}/\mu\text{l}$) (6-hydroxydopaminergic hydrobromide in 0.1% ascorbate saline, Sigma Chemical Co., St. Louis, USA) by two injections ($4\mu\text{l}$ each) into the ascending mesostriatal pathway (4.2 mm posterior to bregma, 1.1 mm lateral to the midline, 7.8 mm below the dura and 4.4 mm posterior

to bregma, 0.9 mm lateral to the midline, 7.8 mm below the dura) near the medial forebrain bundle to lesion dopaminergic innervation to the striatum. The syringe was lowered through the burr hole and the toxin infused at a rate of 1 μ l/min for 4 min, giving a total volume of 8 μ l. The needle was left in the brain for 5 min to prevent back filling along the injection tract and also to allow for diffusion of the toxin away from the injection site, and then retracted. In the same way, controlled rats were infused with a total volume of 8 μ l of saline. The wound was cleansed with saline and sutured.

Rotational behavior

The use of apomorphine, a dopaminergic agonist, allows measurement of rotational asymmetry in unilateral lesioned animals. This measurement was analyzed by placing rats in a white hemispheric plastic rotation bowl (42 cm wide at top and 22 cm deep). Mounted above this bowl was a DVD video camera (Sony, Japan). Individual rats were injected subcutaneously with 0.2 mg/kg apomorphine hydrochloride (Sigma, USA) dissolved in 0.1% ascorbate saline solution. Rotational behavior was then filmed for 30 min in the bowl and the number of ipsiversive and contraversive rotations was quantified by observation of the played film. These tests were carried out 3 or 5 weeks post-lesion. To ensure selection of well-lesioned animals, care was taken to select only animals that responded to apomorphine with at least 7.0 turns/min

Quantification of TH cells

Stereological neuron counts was performed on systematic uniform random sections taken throughout the entire region of interest (spaced approximately 360 μ m apart).

This resulted in a total of 12–16 sections for the striatum and 6–8 sections for the SNc. Estimation of the total number of TH-positive neurons in the SNc was performed using the optical fractionator technique with the aid of StereoInvestigator TM software and a motorized x–y–z stage coupled to a video-microscopy system (MicroBright Field). Analysis was carried out in accordance with previously published protocols (West, 1993; Johansson et al., 2005). Briefly, optical dissectors (area of counting frame 64,000 mm²; guard height 2 µm; spaced 300µm apart in the x-direction, and 200 µm apart in the y-direction) were applied to each section in the series throughout the entire SNc (including pars reticulata and compacta; estimates are reflective of two sides; n=7 for each group). A 40×objective was used to count neurons within the dissectors and to measure postprocessing section thickness. Sampling was optimized to produce a coefficient of error well under the observed biological variability (Gundersen et al., 1999). Given the limited number of positive cells per sections, the cells were identified using a light microscope and manually tallied.

Drug treatment

K252a was dissolved in 0.1% DMSO (200 nm in 5 µl DMSO, Cell Signaling Technology, Inc.). Drug infusions were performed using a microinjector through both cerebral ventricles (from the bregma: anteroposterior, -0.8 mm; lateral, 1.5 mm; depth, 3.5 mm). A volume of 5 µl each was infused over 5 min. K252a was given once per day for 5 consecutive days in successful model and infusion of 1% DMSO served as a vehicle control.

Sample preparation

The majority of rats were decapitated immediately day 7 after successful models selection (at 24h after K252a or DMSO treatment) and then SNc or striatal tissue was isolated and quickly frozen in liquid nitrogen. The SNc and striatum were homogenized in an ice-cold homogenization buffer containing 50 mM 3-(N-morpholino) propanesulphonic acid (MOPS) (Sigma; pH 7.4), 100mMKCl, 320mM sucrose, 50 mM NaF, 0.5 mM MgCl₂, 0.2 mM DTT, 1 mM EDTA, 1 mM EGTA, 1 mM Na₃VO₄ (Sigma), 20 mM sodium pyrophosphate, 20 mM b-phosphoglycerol, 1 mM p-nitrophenyl phosphate (PNPP), 1 mM benzamidine, 1 mM phenylmethylsulphonylfluoride (PMSF) and 5 mg/ml each of leupeptin, aprotinin and pepstatin A.

The homogenates were centrifuged at 800×g for 10 min at 4°C. Supernatants were collected and centrifuged at 100, 000×g for 30 min at 4°C. The supernatants were carefully removed and 500 ml of homogenization buffer containing 1% Triton X-100 Samples were stored at -80°C until use. When necessary, the SNc and striatum were immediately isolated to prepare mitochondrial fractions. All procedures were conducted in a cold room. Non-frozen brain tissue was used to prepare mitochondrial fractions because freezing tissue causes the release of cytochrome c from mitochondria. The SNc and striatal tissues were homogenized in 1:10 (w/v) ice-cold homogenization buffer. The homogenates were centrifuged at 800×g for 10 min at 4°C. The pellets were discarded, and supernatants were centrifuged at 17,000×g for 20 min at 4°C to obtain the cytosolic fraction of the supernatants and the crude mitochondrial

fraction in the pellets.

Nuclear extraction

The homogenates were centrifuged at 800×g for 10 min at 4°C. Cytosolic fractions in the supernatants were collected and protein concentrations were determined. The nuclear pellets were extracted with 20 mM HEPES, pH 7.9, 20% glycerol, 420 mM NaCl, 0.5 mM MgCl₂, 1mMEDTA, 1mMEGTA, 1mMDTT and enzyme inhibitors for 30 min at 4°C with constant agitation. After centrifugation at 12,000×g for 15 min at 4°C, the nuclear fraction in the supernatants was collected and protein concentrations were determined. Samples were stored at -80 °C and were thawed only once.

Immunoprecipitation

Tissue homogenates (400 µg of protein) were diluted 4-fold with 50 mM HEPES buffer, (pH 7.4), containing 10% glycerol, 150 mM NaCl, 1%Triton X-100, 0.5% NP-40 and 1 mM each of EDTA, EGTA, PMSF and Na₃VO₄. Samples were preincubated for 1 h with 20 ml protein A Sepharose CL-4B (Amersham, Uppsala, Sweden) at 4 °C, and then centrifuged to remove proteins adhered non-specifically to protein A. The supernatants were incubated with 1–2 mg of primary antibody for 4 h or overnight at 4°C. Protein A was added to the tube for another 2 h incubation. Samples were centrifuged at 10,000×g for 2 min at 4°C and the pellets were washed three times with immunoprecipitation (IP) buffer for three times. Bound proteins were eluted by boiling at 100°C for 5 min in SDS–PAGE loading buffer and then isolated by centrifuge. The supernatants were used for immunoblot analysis.

Immunoblot

Equal amounts of protein (100 µg/lane) were separated by 7.5%, 10%, 12.5% and 15% SDS-PAGE on polyacrylamide gels and then electrotransferred onto a PVDF membrane (Bio-Rad, Hercules, CA). After blocking for 3 h in Tris-buffered saline (TBS) with 0.1% Tween-20 (TBST) and 3% bovine serum albumin (BSA), membranes were incubated overnight at 4°C with primary antibodies in TBST containing 3% BSA. After washing for 30min in TBS with gentle agitation, the membrane was incubated with biotinylated anti-mouse/rabbit IgG secondary antibody (Vector Laboratories, Burlingame, CA) at room temperature for 2 h. The membrane was then incubated with avidin-biotin complex (Vector Laboratories) and the signals were developed with ECL advanced Western Blotting Detection kit (Amersham, UK). Band intensities were quantified by densitometric analyses using an AxioCam digital camera (ZEISS, CTED PROOF Germany) and a KS400 photo analysis system (Version 3.0).

Immunohistochemistry

Rats were perfusion-fixed with 4% paraformaldehyde in 0.1 M sodium phosphate buffer (pH 7.4) under anesthesia 35 days after 6-OHDA treatment (at 7 days after K252a or DMSO treatment). Brains were removed quickly and further fixed with the same fixation solution at 4 °C overnight. Post-fixed brains were embedded in paraffin, and 5mm coronal sections were obtained using a microtome. Immunoreactivity was determined using the avidin–biotin–peroxidase method. Briefly, sections were de-paraffinized with xylene and rehydrated in ethanol at graded concentrations and rinsed in distilled water. High-temperature antigen retrieval was performed in 1 mM

citrate buffer. To block endogenous peroxidase activity, sections were incubated for 30 min in 1% H₂O₂. After being blocked in 5% (v/v) normal goat serum in PBS for 1 h at 37°C, sections were incubated with a mouse polyclonal antibody against tyrosine hydroxylase (TH, 1:8000) or mouse monoclonal antibody against p-c-Jun (1:50) at 4°C for 24 hours. These sections were then incubated with biotinylated goat-anti-mouse secondary antibody overnight and subsequently with avidin-conjugated horseradish peroxidase for 1 h at 37°C. Finally, sections were incubated with the peroxidase substrate diaminobenzidine (DAB) until desired stain intensity developed.

Antibody and reagents

Mouse monoclonal anti-p-JNKs (sc-6254), rabbit polyclonal anti-MLK3 (sc-13072), mouse monoclonal anti-p-c-Jun (sc-822), rabbit polyclonal anti-Fas L (sc-6237), rabbit polyclonal anti-Fas (sc-716), rabbit polyclonal anti-c-Jun (sc-1694) and rabbit polyclonal anti-14-3-3 (sc-1019) were purchased from Santa Cruz Biotechnology. The monoclonal antibody to phosphoserine was obtained from Alexis Biochemicals. The mouse polyclonal anti-TH, rabbit polyclonal anti-Bax and mouse polyclonal anti-actin were purchased from Sigma. The rabbit polyclonal anti-cytochrome c(#4272), rabbit polyclonal anti-caspase-3(#9662), rabbit polyclonal anti-p-MLK3 (Thr277/Ser281) (#2811), monoclonal antibody of cytochrome c oxidase against subunit IV (#4844) rabbit polyclonal anti-p-ASK1-Thr845(#3765) and rabbit polyclonal anti-ASK1(#3762) were obtained from Cell Signal Biotechnology. The rabbit polyclonal anti-JNK3 antibody (06-749) was obtained from Upstate Biotechnology. The

secondary antibodies used in our experiment were goat anti-mouse IgG and goat anti-rabbit IgG and were purchased Cell Signal Biotechnology.

Statistics

Values are expressed as mean \pm SD and obtained from five or seven independent rats. Statistical analysis of the results was carried out using Student's t-tests or one-way analysis of the variance (ANOVA) followed by Duncan's new multiple range method or Newman-Keuls tests. P-values <0.05 were considered statistically significant.

Results

Effects of K252a on 6-OHDA-treated activation and expression of MLK3 and ASK1

To explore the effects of K252a on MLK3 and ASK1 activation, we evaluated MLK3, ASK1 activation in the SNc and striatum. MLK3/ASK1 activation and MLK3/ASK1 expression in the tissues from these regions were detected by immunoblot analysis using anti-p-MLK3, anti-MLK3, anti-p-ASK1 and anti-ASK1 antibodies, respectively. As shown in Figures 1A and B, 6-OHDA injection resulted in a remarkable increase of both MLK3 and ASK1 phosphorylation in both regions in the treated and untreated sides as compared with sham control. However, the increase of phosphorylated levels was more obvious in the treated side than that in the untreated one. Meanwhile, total MLK3 and ASK1 protein levels were unchanged in both SNc and striatal regions in all samples. To elucidate whether K252a could inhibit the activation of MLK3 or ASK1 after 6-OHDA lesion, we administered the K252a to 6-OHDA-lesioned rats. As shown in Figures 1A and B, both MLK3 and ASK1 activation in the SNc and striatum of both treated and untreated sides was noticeably attenuated by K252a treatment. Levels of total MLK3 and ASK1 protein were unaffected by K252a. Treatment with DMSO did not affect the increase of MLK3 and ASK1 phosphorylation. Immunoblotting with the anti-actin antibody revealed that similar amounts of proteins were loaded in each lane.

JNK3 activation following 6-OHDA lesion

K252a can inhibit JNK activation in cortical neuron cells (Roux et al., 2002),

therefore, we next examined whether treatment with K252a *in vivo* could decrease JNK3 activation, the downstream kinase of MKK7. The study was carried out by IP with p-JNKs antibody and then IB with JNK3 antibody. Furthermore, similar results were obtained from JNK3 like MLK3 (Figs. 2A,B,C,D). Immunoblotting with an anti-actin antibody revealed that similar amounts of protein were loaded in each lane.

K252a modulated 6-OHDA-induced c-Jun phosphorylation only in the SNc

To elucidate the effects of K252a on the activation and expression of c-Jun, the nuclear substrate of JNK, c-Jun phosphorylation was investigated in 6-OHDA lesioned animals. As indicated in Figures. 3A-B, results of western blots showed that the phosphorylation and expression of c-Jun were significantly increased only in SNc after 6-OHDA injection, and no changes were evident in the striatum. Likewise, as shown in Figures 3C-D p-c-Jun was significantly inhibited only in SNc when 6-OHDA rat was treated with K252a, whereas the same dose of DMSO did not have the same effect. The protein levels of c-Jun were not affected by K252a or DMSO treatment. The decreases of p-c-Jun were also observed in immunohistochemistry examination(Fig. 3Eg-h). Similar changes of p-c-Jun occurred in untreated side (data not shown). However, these changes were not found in the striatum (Figs. 3F).

K252a attenuated 6-OHDA-induced increasing Fas L expression in the SNc and striatum.

To investigate whether the Fas receptor-mediated pathway is involved in the death profile induced by 6-OHDA lesion, Fas L and Fas expression was analyzed by western blot. As indicated in Fig.4A, Fas L expression was significantly increased in

both SNc and striatum following 6-OHDA lesion, whereas no significant changes were observed in Fas expression. However, application of K252a could diminish the increasing Fas L expression induced by 6-OHDA lesion. Animals treated with DMSO showed no changes in the expression of Fas L. Fas protein levels were not affected by either K252a or DMSO (Fig4B).

K252a attenuated the decreased interaction of Bax and 14-3-3, phosphorylation of 14-3-3, Bax translocation, and the release of cytochrome c in SNc and striatum induced by 6-OHDA lesion

To study the involvement of mitochondrial pathways in the cell death after 6-OHDA lesion, 14-3-3 phosphorylation, Bax and 14-3-3 interactions, and Bax and cytochrome c expression were evaluated in the mitochondria and cytosol by IB and IP. As indicated in Figure 5A, B, results of reciprocal IP indicated that 14-3-3 phosphorylation was significantly increased in the SNc and striatum post 6-OHDA lesion, whereas 14-3-3 protein levels were not affected. Meanwhile, interactions between Bax and 14-3-3 were decreased corresponding to the increased phosphorylation of 14-3-3. The disassociated Bax could translocate from cytosol to mitochondria and facilitate cytochrome *c* release.

Recent studies have indicated that JNK can phosphorylates the 14-3-3 protein thereby promoting the disassociation of Bax from 14-3-3 and subsequent translocation to the mitochondria. Since K252a inhibited JNK activation, we hypothesized that inhibition of the JNK signaling pathway could attenuate the decreased interaction of Bax and 14-3-3, phosphorylation of 14-3-3 and subsequently prevent Bax

translocation and the release of cytochrome *c*. As shown in Figure. 5C, D, K252a inhibited phosphorylation of 14-3-3 and increased the association of Bax and 14-3-3 in the treated side comparing to the sham group. The inhibitory effects of K252a on the Bax translocation was demonstrated by the decreased Bax in the mitochondrial fraction prepared from the tissues of K252a-treated rat (Fig. 5E). Similar changes occurred in SNc of treated side, as well as in both SNc and striatum of untreated side (data not shown). In the mitochondrial fraction immunoreactivity of cytochrome *c* was evident as a single band with a molecular mass of 15 kDa both in SNc and striatum. Mitochondrial cytochrome *c* was decreased, corresponding to a significant increase in the cytosolic fraction in the 6-OHDA-treated striatum (Fig. 5G). K252a could also block the release of cytochrome *c* to the cytosol in 6-OHDA rats treated with K252a, while these effects of K252a were not observed in 6-OHDA-lesioned rats and DMSO-treated rats (Fig. 5G). To further validate whether other mitochondria proteins were released from the mitochondria, we examined cytochrome *c* oxidase level in the cytosolic and mitochondria fractions respectively using an anti-cytochrome *c* oxidase subunit IV antibody. The cytochrome *c* oxidase subunit IV was detected only in the mitochondrial fraction, but not in the cytosolic fraction in sham, 6-OHDA, DMSO and K252a groups, which suggested that cytochrome *c* oxidase was not related with the release cytochrome from mitochondria. Similar effects were taken place in SNc of treated side, as well as both in SNc and striatum of untreated side (data not shown).

Effects of K252a on 6-OHDA-induced caspase-3 activation in the SNc and

striatum

Caspase-3 is a potent effector of apoptosis triggered via several pathways in a variety of mammalian cell types. Caspase 3 is one of the most important caspases activated by cytochrome c in the cytochrome c-dependent apoptosis pathways. As visualized via western blot, caspase-3 was activated both in the SNc and striatum in 6-OHDA injury. Treatment with K252a inhibited the 6-OHDA-induced increase in caspase-3 activation in both brain regions (Fig. 6A, B, C, D). Immunoblotting with an anti-actin antibody revealed that similar amounts of proteins were loaded in each lane.

K252a attenuated 6-OHDA-induced striatal dopaminergic terminal loss and nigral neuron death

In order to explore whether the inhibition of K252a on MLK3/JNK3 activation can reduce the programmed cell death induced by 6-OHDA neurotoxicity, we first examined the effect of K252a on TH-positive neurons in SNc of 6-OHDA rat. As shown in Figure 7A, 6-OHDA induced marked nigral cell death. However, administration of K252a clearly rescued the neurodegeneration caused by 6-OHDA. These changes were specific to the SNc of treated side (Fig. 7B), as there was no cell death in the SNc of untreated side. The results indicated that K252a was capable of protecting neurons against 6-OHDA-induced injury.

TH immunostaining in the striatum was assessed as an indication of dopaminergic axon and pre-synaptic integrity. The results revealed K252a treatment minimized the decreased densities of TH-IR in the caudate-putamen (CP) region of the striatum (Fig. 7C d, b), while the solvent control did not have such effect (Fig. 7C d, c). There

was no difference in TH-IR between 6-OHDA and solvent control-treated rats. No change was noted in the striatum of untreated side (Fig. 7 C, D).

Apomorphine-induced rotational behavior

In the experiment, 6-OHDA-treated rats showed apomorphine-induced rotations compared with sham. A significant reduction in apomorphine-induced rotations was seen in all groups injected K252a, whereas the animals exhibited no markedly reduction in apomorphine-induced rotations after 1 week DMSO treatment (Fig.8).

Discussion

Various mechanisms have been proposed to account for the neurodegeneration induced by 6-OHDA. Early studies suggested that 6-OHDA-induced neuronal damage *in vitro* was due to the activation of MAPK signaling pathway (Bozyczko-Coyne, et al., 2002; Wu and Frucht, 2005). A large and growing of evidence suggests that the JNK3 pathway can function in a pro-apoptotic manner. The activation of the MAPK family subunit JNKs induced neuronal death in the SNc, and JNKs-deficient rats exhibited resistance to 6-OHDA-induced injury (Wu and Frucht, 2005). JNK3 is predominantly expressed in the brain and is most consistently associated with neuronal death (Keramaris et al., 2005). Previous studies have shown that disruption of the neural-specific *Jnk3* gene, but not *Jnk1* or *Jnk2*, highly renders mice resistant to glutamate excitotoxicity (Yang et al., 1997). These studies suggest that JNK3 may have a preferential role in stress-induced neuronal apoptosis. Moreover, a recent study has revealed that neural-specific JNK3 plays a critical role in c-Jun phosphorylation and apoptosis *in vivo*, whereas JNK1 and JNK2 deficiency do not appear to have the same effect (Kuan et al., 2003), suggesting that JNK3 is a potential target for neuroprotective therapies (Keramaris et al., 2005).

All MLK family members and ASK1 regulate the JNK signaling pathway by phosphorylating MKK4 and MKK7. MKK4 and MKK7 are dual-specificity kinases that phosphorylate tyrosine and threonine residues in the catalytic domains of JNKs (Davis, 2000). Our previous study also suggested that both MLK3 and ASK1 can activate JNK3 by serial activations MKK7 (Pan et al., 2005), and that JNK3 is

involved in the neuronal death induced by ischemia /reperfusion (Pan et al., 2005; Pei et al., 2006). However, whether the same mechanism existed in the 6-OHDA-induced brain injury remains unknown. As a matter of fact, results from western blot indicated that MLK3, ASK1 and JNK3 phosphorylation were increased in 6-OHDA rats. It is therefore possible that suppressing the over-activation of JNK signaling pathway can effectively protect neurons against 6-OHDA-induced neuronal damage. K252a is a demonstrated neuroprotective compound which has been shown inhibit of MLK3 activity and activate PI3K and MEK signaling pathways through interactions with distinct targets (Roux et al., 2002). Increasing evidence indicates that the K252a family blocks the JNK stress signaling cascade and promotes cell survival. Our previous studies also indicated ASK1, another upstream activator of JNK, activation can be inhibited by PI3K/AKT1 phosphorylation (Wang et al., 2007). However, the possible mechanism underlying the protective effects of K252a in 6-OHDA-lesioned rats remains unclear. In the present study, we found that K252a attenuated both MLK3 and ASK1 activation and subsequently attenuated the activation of MLK/JNK3 and ASK1/JNK3. Furthermore, our unpublished findings has identified 6-OHDA lesion can activate AKT1 and ERK1, consisting with the results of Signore et al (Signore et al., 2006). Maybe K252a directly inhibits MLK3 activation and indirectly inhibits ASK1 activation via AKT pathway. The formation of distinct signaling complexes is required to regulate the specificity of signal transduction pathways; it may be possible that MLK3 and ASK1 were in a respective specific complex of MLK3–MKK–JNK3 cascade and ASK1–MKK–JNK3 cascade that subsequently regulated JNK3 activation.

However, other mechanisms may be also involved in JNK3 activation in 6-OHDA-induced cell death.

JNK may promote neuronal death by regulating the activation of downstream pathways, i.e. nuclear or non-nuclear pathway. However, it is still unclear that 6-OHDA-induced dopaminergic cell death is mediated by which pathways.

Activated JNK can regulate various nuclear substrates, such as c-Jun, as well as cytosol substrates. In fact, previous studies suggest that c-Jun plays an important role in neuronal death under *in vitro* and *in vivo* conditions (Pei et al., 2006). Activated JNK phosphorylates the transcription factor c-Jun, and the subsequent increasing of AP-1 activity modulates the transcription of a number of genes such as Fas ligand (Fas L) (Faris et al., 1998). Western blot results showed that treatment with K252a could inhibit c-Jun phosphorylation induced by 6-OHDA lesion only in SNc but not striatum. Similar results were also found in immunohistochemistry. This is because the c-Jun only expresses in cell nucleus in both SNc and striatum, but the dopaminergic neuron bodies only exist in SNc. Therefore, the changes mentioned above are only found in the SNc. In addition, K252a can also significantly decrease the expression of Fas L induced by 6-OHDA lesion. Taken together, these results suggest that the nuclear signal pathways mediated by JNK3 activation is involved in dopaminergic neuronal death induced by 6-OHDA.

Apart from nuclear pathway, JNK can also promote cell death by regulating the activation of some non-nuclear substrates, such as Bcl-2 family members. Recently, it has been demonstrated that Bax plays an essential role in inducing apoptosis in

response to stress stimuli (Finkelstein et al., 2000; Zong et al., 2001). A substantial proportion of Bax is bound to 14-3-3 proteins in the cytosol of normal cells. Under stress, Bax dissociates from 14-3-3 and redistributes to mitochondria (Nomura et al., 2003). After translocation to mitochondria, Bax induces cytochrome *c* release either by forming a pore in the outer mitochondrial membrane or by opening other channels (Kuwana et al., 2002). Recent studies have also shown that 14-3-3 proteins prevent cell death through sequestration of Bax (Nomura et al., 2003). Since JNK3 could be activated by 6-OHDA lesion, we suppose that the activation of JNK3 may enhance the phosphorylation of 14-3-3 protein and promote Bax translocation to the mitochondria, and cause releasing cytochrome *c* and increasing caspase-3 activation. This speculation was proved by the results from our experiments. Meanwhile, treatment with K252a prevented Bax translocation to mitochondria and diminished the release of cytochrome *c* and the activation of caspase-3, which ultimately attenuated mitochondria-mediated apoptosis. It is demonstrated that the non-nuclear pathway, i.e. the mitochondria-dependent mediated by JNK3 activation also participates in 6-OHDA-induced cell death.

Increasing evidence indicates that the K252a blocks the JNK stress signaling cascade and promotes cell survival.(Roux et al., 2002; Pan et al., 2005). Here, application of K252a attenuated not only the activation of MLK3/JNK3 but also ASK1/JNK3 activation. Furthermore, K252a inhibited the recruitment of both nuclear and non-nuclear of JNK pathways induced by 6-OHDA lesion. Importantly, we found that treatment with K252a improved apomorphine-induced rotational behavior in

6-OHDA lesioned rats. The results from immunohistochemistry provided high fidelity to our hypothesis that application of K252a may also rescue dopaminergic terminals as well as SNc cell bodies from degeneration. However it was interesting to note that the changes to the examined protein kinases were not exclusive to the treated side both in SNc and striatum, and similar alterations were noted in the untreated side. One possibility is that unilateral 6-OHDA lesion may slowly affect untreated side and kinase activation occurred earlier than histological alterations in untreated side. Another interesting thing is that CEP1347, an ethylthiomethyl derivative of K252a that blocks MLK3 are effective in animal model systems, they have been ineffective in clinical trials of PD (Waldmeier et al., 2006). One possibility is that any drugs with single target are not recognized as favorable compounds comparing with manifold targets drug for PD (Johnston and Brotchie 2006). For example, CEP1347 did not affect p-Erk or p-Akt levels (Harris et al., 2002) as well as p-ASK1 (Maroney et al., 2001). However, K252a could inhibit the JNK3 activation through different pathways.

Taken together, in the unilateral 6-OHDA-lesioned rat model, we have mainly elucidated the presence of JNK3 activation and neuronal injury specially mediated by MLK3 activation. These results strongly suggest a role for MLK3 and ASK1 mediated neuronal death in 6-OHDA-lesioned regions and provide further support for a role of JNK signaling in 6-OHDA lesion. 6-OHDA induced the activation of MLK3/JNK3 and ASK1/JNK3 signaling cascade and subsequently activated JNK down-stream signaling pathways, ultimately resulting in neuronal death. K252a can attenuate both activation of MLK3/JNK3 and ASK1/JNK3 and then inhibit the

MOL#38463

recruitment of both nuclear and non-nuclear of JNK pathways. Importantly, K252a exhibited neuroprotective effects on rat dopaminergic neurons exposed to the 6-OHDA toxin. In view of the causal role of JNK3 pathway in neuronal apoptosis (Bozyczko-Coyne et al., 2002; Tsuruta et al., 2004), targeting the JNK pathway for therapeutic benefit may be a therapeutically attractive strategy. Thus, the present study clarifies the regulatory mechanisms within the MLK3/JNK3 and ASK1/JNK3 signaling cascade involving in 6-OHDA lesion.

Reference

- Bozyczko-Coyne D, Saporito MS, Hudkins RL (2002) Targeting the JNK pathway for therapeutic benefit in CNS disease. *Curr Drug Targets CNS Neurol Disord* **1**:31-49.
- Brunet A, Bonni A, Zigmond MJ, Lin MZ, Juo P, Hu LS, Anderson MJ, Arden KC, Blenis J, Greenberg ME (1999) Akt promotes cell survival by phosphorylating and inhibiting a Forkhead transcription factor. *Cell* **96**:857-868.
- Choi WS, Eom DS, Han BS, Kim WK, Han BH, Choi EJ, Oh TH, Markelonis GJ, Cho JW, Oh YJ (2004) Phosphorylation of p38 MAPK induced by oxidative stress is linked to activation of both caspase-8- and -9-mediated apoptotic pathways in dopaminergic neurons. *J Biol Chem* **279**:20451-20460.
- Davis RJ (2000) Signal transduction by the JNK group of MAP kinases. *Cell* **103**:239-252.
- Eminell S, Klettner A, Roemer L, Herdegen T, Waetzig V (2004) JNK2 translocates to the mitochondria and mediates cytochrome c release in PC12 cells in response to 6-hydroxydopamine. *J Biol Chem* **279**:55385-55392.
- Faris M, Latinis KM, Kempiak SJ, Koretzky GA, Nel A (1998) Stress-induced Fas ligand expression in T cells is mediated through a MEK kinase 1-regulated response element in the Fas ligand promoter. *Mol Cell Biol* **18**:5414-5424.
- Finkelstein DI, Stanic D, Parish CL, Tomas D, Dickson K, Horne MK (2000) Axonal sprouting following lesions of the rat substantia nigra. *Neuroscience* **97**:99-112.
- Gallo A, Cuzzo C, Esposito I, Maggiolini M, Bonfiglio D, Vivacqua A, Garramone

- M, Weiss C, Bohmann D, Musti AM (2002) Menin uncouples Elk-1, JunD and c-Jun phosphorylation from MAP kinase activation. *Oncogene* **21**:6434-6445.
- Gundersen HJ, Jensen EB, Kieu K, Nielsen J (1999) The efficiency of systematic sampling in stereology--reconsidered. *J Microsc* **193**:199-211.
- Hanrott K, Gudmunsen L, O'Neill MJ, Wonnacott S (2006) 6-hydroxydopamine-induced apoptosis is mediated via extracellular auto-oxidation and caspase 3-dependent activation of protein kinase Cdelta. *J Biol Chem* **281**:5373-5382.
- Harris CA, Deshmukh M, Tsui-Pierchala B, Maroney AC, Johnson EM Jr (2002) Inhibition of the c-Jun N-terminal kinase signaling pathway by the mixed lineage kinase inhibitor CEP-1347 (KT7515) preserves metabolism and growth of trophic factor-deprived neurons. *J Neurosci* **22**:103-113.
- Irving EA, Bamford M (2002) Role of mitogen- and stress-activated kinases in ischemic injury. *J Cereb Blood Flow Metab* **22**:631-647.
- Jiang H, Ren Y, Zhao J, Feng J (2004) Parkin protects human dopaminergic neuroblastoma cells against dopamine-induced apoptosis. *Hum Mol Genet* **13**:1745-1754.
- Johansson S, Lee IH, Olson L, Spenger C (2005) Olfactory ensheathing glial co-grafts improve functional recovery in rats with 6-OHDA lesions. *Brain* **128**:2961-2976.
- Johnston TH, Brotchie JM (2006) Drugs in development for Parkinson's disease: an update. *Curr Opin Investig Drugs* **7**:25-32.

MOL#38463

- Kaneko M, Saito Y, Saito H, Matsumoto T, Matsuda Y, Vaught JL, Dionne CA, Angeles TS, Glicksman MA, Neff NT, Rotella DP, Kauer JC, Mallamo JP, Hudkins RL, Murakata C (1997) Neurotrophic 3,9-bis[(alkylthio)methyl]-and-bis(alkoxymethyl)-K-252a derivatives. *J Med Chem* **40**:1863-1869.
- Keramaris E, Vanderluit JL, Bahadori M, Mousavi K, Davis RJ, Flavell R, Slack RS, Park DS (2005) c-Jun N-terminal kinase 3 deficiency protects neurons from axotomy-induced death in vivo through mechanisms independent of c-Jun phosphorylation. *J Biol Chem* **280**:1132-1141.
- Kuan CY, Whitmarsh AJ, Yang DD, Liao G, Schloemer AJ, Dong C, Bao J, Banasiak KJ, Haddad GG, Flavell RA, Davis RJ, Rakic P (2003) A critical role of neural-specific JNK3 for ischemic apoptosis. *Proc Natl Acad Sci U S A* **100**:15184-15189.
- Kuwana T, Mackey MR, Perkins G, Ellisman MH, Latterich M, Schneider R, Green DR, Newmeyer DD (2002) Bid, Bax, and lipids cooperate to form supramolecular openings in the outer mitochondrial membrane. *Cell* **111**:331-342.
- Maroney AC, Finn JP, Connors TJ, Durkin JT, Angeles T, Gessner G, Xu Z, Meyer SL, Savage MJ, Greene LA, Scott RW, Vaught JL (2001) Cep-1347 (KT7515), a semisynthetic inhibitor of the mixed lineage kinase family. *J Biol Chem* **276**:25302-25308.
- Mohit AA, Martin JH, Miller CA (1995) p493F12 kinase: a novel MAP kinase

- expressed in a subset of neurons in the human nervous system. *Neuron* **14**:67-78.
- Nomura M, Shimizu S, Sugiyama T, Narita M, Ito T, Matsuda H, Tsujimoto Y (2003) 14-3-3 Interacts directly with and negatively regulates pro-apoptotic Bax. *J Biol Chem* **278**:2058-2065.
- Ouyang M, Shen X (2006) Critical role of ASK1 in the 6-hydroxydopamine-induced apoptosis in human neuroblastoma SH-SY5Y cells. *J Neurochem* **97**:234-244.
- Ozes ON, Mayo LD, Gustin JA, Pfeffer SR, Pfeffer LM, Donner DB (1999) NF-kappaB activation by tumour necrosis factor requires the Akt serine-threonine kinase. *Nature* **401**:82-85.
- Pan J, Zhang QG, Zhang GY (2005) The neuroprotective effects of K252a through inhibiting MLK3/MKK7/JNK3 signaling pathway on ischemic brain injury in rat hippocampal CA1 region. *Neuroscience* **131**:147-159.
- Pei DS, Wang XT, Liu Y, Sun YF, Guan QH, Wang W, Yan JZ, Zong YY, Xu TL, Zhang GY (2006) Neuroprotection against ischaemic brain injury by a GluR6-9c peptide containing the TAT protein transduction sequence. *Brain* **129**:465-179.
- Plesnila N, Zinkel S, Le DA, Amin-Hanjani S, Wu Y, Qiu J, Chiarugi A, Thomas SS, Kohane DS, Korsmeyer SJ, Moskowitz MA (2001) BID mediates neuronal cell death after oxygen/ glucose deprivation and focal cerebral ischemia. *Proc Natl Acad Sci U S A* **98**:15318-15323.
- Roux PP, Dorval G, Boudreau M, Angers-Loustau A, Morris SJ, Makkerh J, Barker PA (2002) K252a and CEP1347 are neuroprotective compounds that inhibit

- mixed-lineage kinase-3 and induce activation of Akt and ERK. *J Biol Chem* **277**:49473-49480.
- Signore AP, Weng Z, Hastings T, Van Laar AD, Liang Q, Lee YJ, Chen J (2006) Erythropoietin protects against 6-hydroxydopamine-induced dopaminergic cell death. *J Neurochem* **96**(2):428-443.
- Tischler AS, Ruzicka LA, Dobner PR (1991) A protein kinase inhibitor, staurosporine, mimics nerve growth factor induction of neurotensin/neuromedin N gene expression. *J Biol Chem* **266**:1141-1146.
- Tsuruta F, Sunayama J, Mori Y, Hattori S, Shimizu S, Tsujimoto Y, Yoshioka K, Masuyama N, Gotoh Y (2004) JNK promotes Bax translocation to mitochondria through phosphorylation of 14-3-3 proteins. *EMBO J* **23**:1889-1899.
- Waldmeier P, Bozyczko-Coyne D, Williams M, Vaught JL (2006) Recent clinical failures in Parkinson's disease with apoptosis inhibitors underline the need for a paradigm shift in drug discovery for neurodegenerative diseases. *Biochem Pharmacol* **72**:1197-1206.
- Wang LH, Besirli CG, Johnson EM Jr (2004) Mixed-lineage kinases: a target for the prevention of neurodegeneration. *Annu Rev Pharmacol Toxicol* **44**:451-474.
- Wang Q, Zhang QG, Wu DN, Yin XH, Zhang GY (2007) Neuroprotection of selenite against ischemic brain injury through negatively regulating early activation of ASK1/JNK cascade via activation of PI3K/AKT pathway. *Acta Pharmacol Sin* **28**:19-27.
- West MJ (1993) New stereological methods for counting neurons. *Neurobiol Aging*

14:275-285.

Wilhelm M, Xu Z, Kukekov NV, Gire S, Greene LA (2007) Proapoptotic Nix activates the JNK pathway by interacting with POSH and mediates death in a Parkinson disease model. *J Biol Chem* **282**:1288-1295.

Wu SS, Frucht SJ (2005) Treatment of Parkinson's disease: what's on the horizon?. *CNS Drugs* **19**:723-743.

Yang DD, Kuan CY, Whitmarsh AJ, Rincon M, Zheng TS, Davis RJ, Rakic P, Flavell RA (1997) Absence of excitotoxicity-induced apoptosis in the hippocampus of mice lacking the Jnk3 gene. *Nature* **389**:865-870.

Zhang GY, Zhang QG (2005) Agents targeting c-Jun N-terminal kinase pathway as potential neuroprotectants. *Expert Opin Investig Drugs* **14**:1373-1383.

Zong WX, Lindsten T, Ross AJ, MacGregor GR, Thompson CB (2001) BH3-only proteins that bind pro-survival Bcl-2 family members fail to induce apoptosis in the absence of Bax and Bak. *Genes Dev* **15**:1481-1486.

Footnotes

a) This work was supported by grants from the National Program of Basic Research (2006CB500706) of China, National Natural Science Fund (30471918, 30570637), Shanghai Key Project of Basic Science Research (04DZ14005) and Program for Outstanding Medical Academic Leader (LJ 06003).

b) Address correspondence to: Dr. Sheng-Di Chen, *Department of Neurology and Neuroscience Institute, Ruijin Hospital, Shanghai Jiao-Tong University School of Medicine, Shanghai 200025, P.R.China; #Institute of Health Science, Shanghai Institutes for Biological Sciences (SIBS), Chinese Academy of Sciences (CAS) & Shanghai Jiao-Tong University School of Medicine, Shanghai 200025, P.R.China. Tel: +86-21-6445-7249; Fax: +86-21-6445-7249; E-mail: chen_sd@medmail.com.cn

Legends for Figures

Fig. 1. 6-OHDA-induced alteration of MLK3/ASK1 and the effects of K252a on

p-MLK3/P-ASK1. Extracts were obtained from SNc and striatum regions from sham or 6-OHDA lesion rats. Representative image of immunoblotting using anti-phospho-MLK3 antibody, anti-MLK3 antibody anti-phospho-ASK1 antibody or conventional anti-ASK1 antibody using extracts from SNc and striatum (A). Prevention of 6-OHDA-induced phosphorylation of MLK3 and ASK1 by treatment with K252a (C). Representative image of immunoblotting with anti-phospho-MLK3, anti-MLK3, anti-phospho-ASK1 antibody or anti-ASK1 antibody using cell extracts. Bands corresponding to MLK3, p-MLK3, ASK1 and p-ASK1, were scanned and the intensities were represented as folds vs. sham control. Data were expressed as mean±S.D. from four independent animals (n=5) and expressed as power of control (sham-operated) animals (B, D). ^a*p* <0.05 vs. sham-treated side; ^b*p* <0.05 vs. 6-OHDA-treated side; ^c*p* <0.05 vs. 6-OHDA-treated side; ^d*p* <0.05 vs. 6-OHDA+DMSO treated side; ^e*p* <0.05 vs. 6-OHDA+DMSO treated side; ^f*p* <0.05 vs. 6-OHDA+DMSO untreated side.

Fig.2. Change in JNK3 phosphorylation from sham and 6-OHDA lesion model and effects of k252a on 6-OHDA-induced activation of JNK3.

JNK3 was examined by immunoblotting, while p-JNK3 was examined by immunoprecipitation and immunoblot analysis in the cytosol fraction from SNc or striatum (A, C). Bands corresponding to JNK3 and p-JNK3 were scanned and the intensities were represented as folds vs. sham-treated side. JNK3 activation were

inhibited by K252a in compared with the rat treated with vehicle DMSO both in SNc and striatum(C).Data were expressed as mean±S.D. from four independent animals (n=5) and expressed as power of sham animals (B, D). ^a*p* <0.05 vs. sham-treated side; ^b*p* <0.05 vs. 6-OHDA -treated side. ^c*p* <0.05 vs. 6-OHDA treated side; ^d*p* <0.05 vs. 6-OHDA+DMSO treated side; ^e*p* <0.05 vs. 6-OHDA+DMSO treated side; ^f*p* <0.05 vs. 6-OHDA+DMSO untreated side.

Fig.3. K252a can modulate 6-OHDA-induced c-Jun phosphorylation only in the SNc. A, immunoblotting analysis of p-c-Jun and c-Jun with anti-p-c-Jun and anti-c-Jun antibodies. C, Effects of treatment with K252a on the increased p-c-Jun induced by 6-OHDA lesion. B, D bands were scanned and the intensities were determined by optical density (O.D.) measurement. Data are the mean ±SD and were expressed as folds vs. sham-treated side(n=5). ^a*p* <0.05 vs. sham-treated side; ^b*p* <0.05 vs. 6-OHDA-treated side; ^c*p* <0.05 vs. 6-OHDA+DMSO treated side; ^d*p* <0.05 vs. 6-OHDA+DMSO non-treated side. E,F, Immunohistochemical staining of p-c-Jun in SNc and striatum. Example of immunohistochemical staining sections of SNc and striatum from sham-treated side [E (a,b), F(a,c)], rats subjected 6-OHDA-induced lesion [E (c,d), F(d)], and rats subjected DMSO [E (e,f), F(e)]or K252a following 6-OHDA lesion [E (g,h), F(f)]. Data were obtained from six independent animals in each experimental group, and the results of a typical experiment are presented. Scale bars: E(a,c,e,g), F(a,b) =200 μm; E(b,d,f,h), [C(c,d,e,f) =20 μm.

Fig.4 K252a diminished the increased protein level of FasL in rat SNc and striatum. A and B, change of the expression of FasL and Fas in SNc and striatum,

derived from sham, saline or 6-OHDA lesion rats. C.D effects of K252a on the expression FasL and Fas following 6-OHDA lesion. Samples were probed with anti-FasL or anti-Fas antibodies. Bands were scanned and the intensities were determined by optical density (O.D.) measurement. Data are the mean \pm SD and are expressed as folds vs. sham-treated side. ^a*p* <0.05 vs. sham-treated side; ^b*p* <0.05 vs. 6-OHDA-treated side. ^c*p* <0.05 vs. 6-OHDA treated side; ^d*p* <0.05 vs. 6-OHDA+DMSO treated side; ^e*p* <0.05 vs. 6-OHDA+DMSO treated side; ^f*p* <0.05 vs. 6-OHDA+DMSO untreated side (n = 5).

Fig.5 Treatment with K252a attenuated the mitochondrial death-signaling pathway. A, Change about phosphorylation of 14-3-3 and the interaction of Bax and 14-3-3 in striatum derived from sham-treated rats or rats submitted lesion. C, Effects of K252a on the increased phosphorylation of 14-3-3 and the decreased interaction of Bax and 14-3-3 induced by 6-OHDA-induced lesion in striatum of treated side. E, Effects of K252a on the increased Bax translocation to mitochondria induced by 6-OHDA lesion in striatum of treated side. G, Effects of K252a on the redistribution of cytochrome c in cytosol and mitochondria induced by 6-OHDA lesion in striatum of treated side. Cytochrome oxidase 4 (COX4) was strongly expressed in the mitochondrial fraction and did not decrease following 6-OHDA lesion, but virtually no immunoreactivity was seen in the cytosolic fraction. Bands corresponding to 14-3-3, Bax, cytochrome c and cytochrome oxidase 4 were scanned and the intensities were represented as folds versus striatum of sham-treated side. Data are the mean \pm SD. ^a*p* <0.05 vs. versus striatum of sham-treated side; ^b*p* <0.05 vs. 6-OHDA treated

side(n=5).

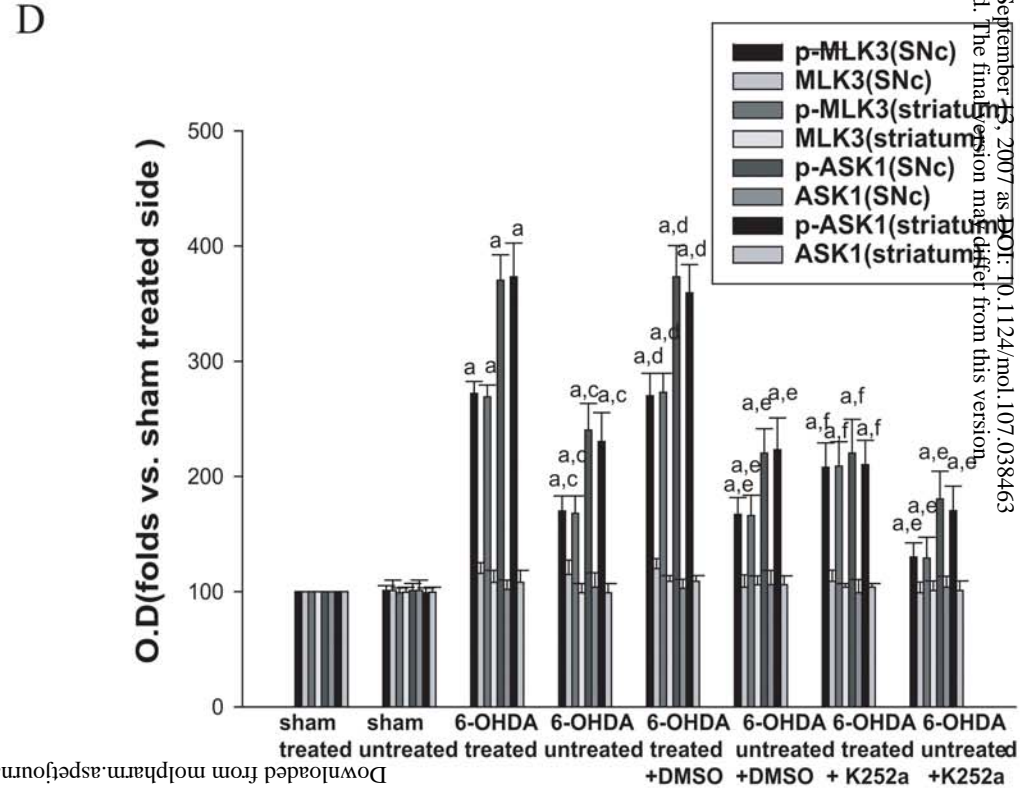
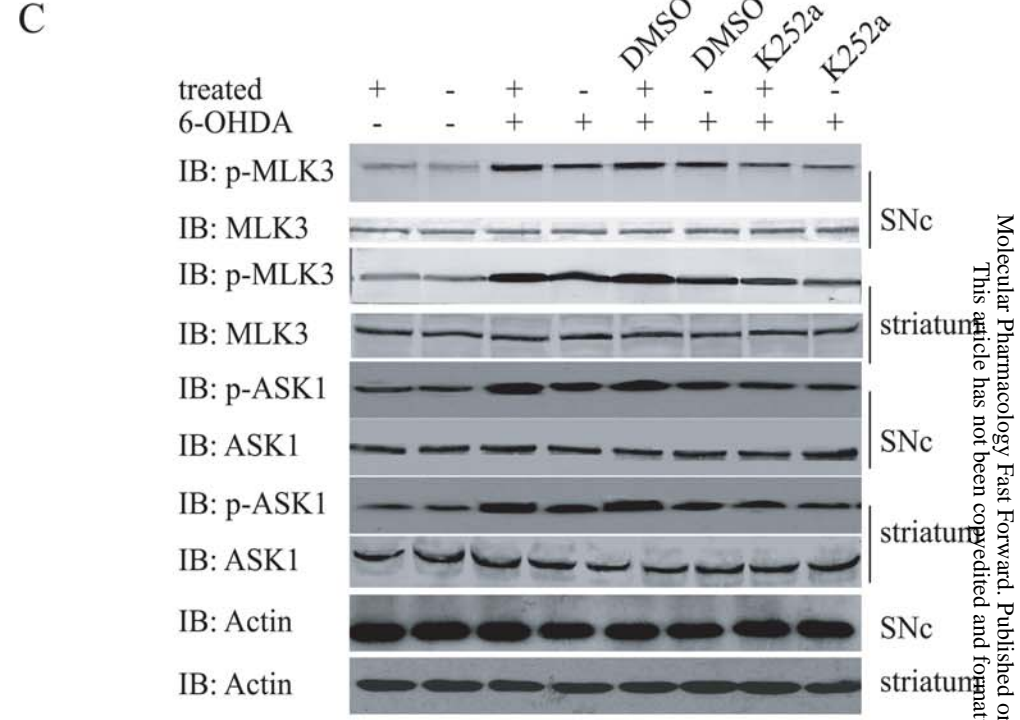
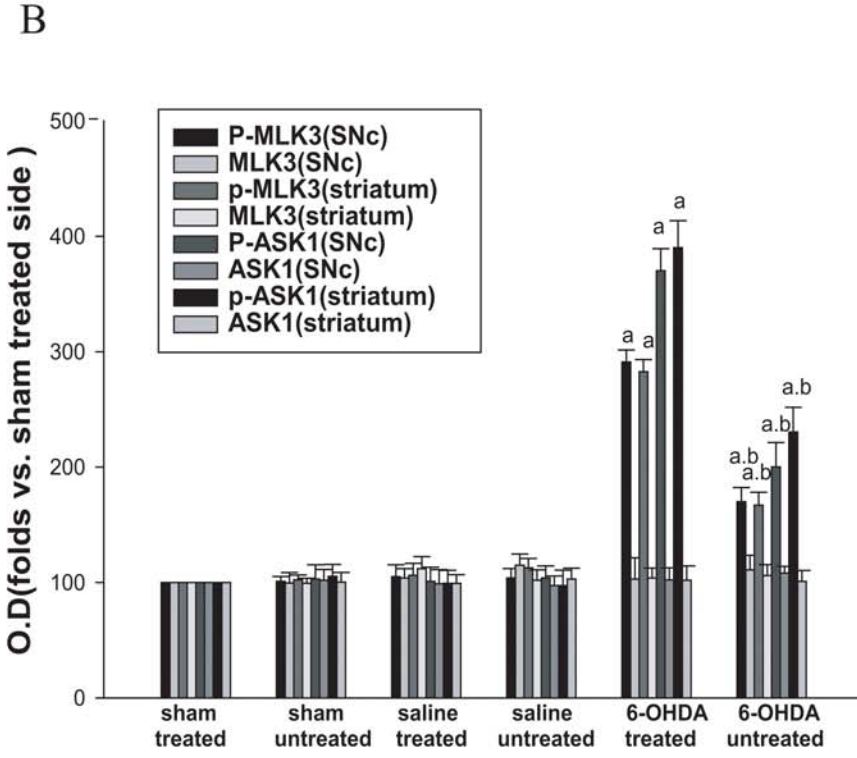
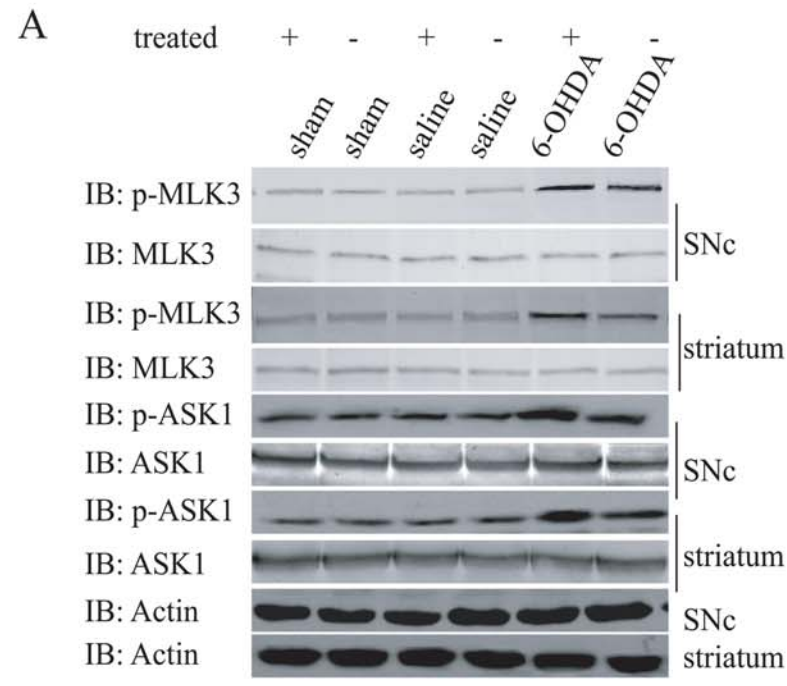
Fig.6 K252a decreased the activation of caspase-3 in cytosol in rat SNc and striatum. A, cleaved caspase-3 and the protein levels of caspase-3 were examined by immunoblotting analysis. C, bands corresponding to caspase-3 were scanned and the intensities were represented as folds vs. sham-treated side. Data are the mean±SD and were expressed as folds vs. sham-treated side. ^a*p* <0.05 vs. sham-treated side; ^b*p* <0.05 vs. 6-OHDA-treated side. ^c*p* <0.05 vs. 6-OHDA treated side; ^d*p* <0.05 vs. 6-OHDA+DMSO treated side; ^e*p* <0.05 vs. 6-OHDA+DMSO treated side; ^f*p* <0.05 vs. 6-OHDA+DMSO untreated side (n = 5).

Fig. 7 K252a attenuates 6-OHDA lesion-induced striatal DA terminal loss and dopaminergic neuron death in the SNc. Example of TH-stained sections of the SNc in sham group [A(a,a-1,a-2)], and rats subjected 6-OHDA-induced lesion [A(b,b-1,b-2)], administration of the vehicle [A(c,c-1,c-2)] and K252a (200 nM in 5 µl DMSO) following lesion [A(d,d-1,d-2,)]. Data were obtained from 7 independent animals and on typical experiment was presented. Quantitative analysis of the protective effects of K252a against 6-OHDA-induced rat model of nigrostriatal damage (B). Survivals of TH-positive cells in SNc were determined 7days after injection K252a. Data were mean±S.D. (n=7 animals per group), ^a*p* <0.05 vs. sham. ^b*p* <0.05 vs. 6-OHDA+DMSO group. C, D assessment of axon terminal density in the striatum. When compared to K252a treated rats several DMSO-treated rats following 6-OHDA lesion showed marked reduction in TH-IR in the CP region of lesioned side (c,d). At the same time, there was considerable variability in the amount of TH-IR

reduction between sham and 6-OHDA-lesion rats of treated side (a,b). Contrarily, immunostaining of the CP region showed no differences in the different groups of non- treated side (a,b,c,d) ((d-1,d-2) are higher magnifications). Scale bars: A(a-1,b-1,c-1,d-1), C(a,b,c,d) =2000 μ m; A(a-1,b-1,c-1,d-1) =200 μ m; A(a-2, b-2, c-2,d-2), C(d-1,d-2) =20 μ m.

Fig.8. Changes in drug-induced rotational behavior in 6-OHDA lesioned rats that have been treated with K252a. Rats were intraperitoneal injected with 0.2mg/kg apomorphine. The number of full 360° rotations was also counted after the administration of apomorphine (for 30 min). Rotational behavior induced by apomorphine was assessed at 21 and 36 days, respectively. Net turning behavior = (number of turns on treated side-number of turns untreated side) was calculated. K252a caused significant reduction of apomorphine-induced rotations compared to animals given only the same dose of DMSO, whereas DMSO could not improve apomorphine-induced rotations compared to rats given 6-OHDA. All group comparisons performed were all statistically significant (one way ANOVA, $F=104.74, p<0.05$, all group comparisons post hoc $p\leq 0.05$). Vertical columns indicate mean \pm standard error (s) of each group. All groups n=7. ^a $p < 0.05$ vs. sham, ^b $p < 0.05$ vs. 6-OHDA+DMSO

Fig. 1



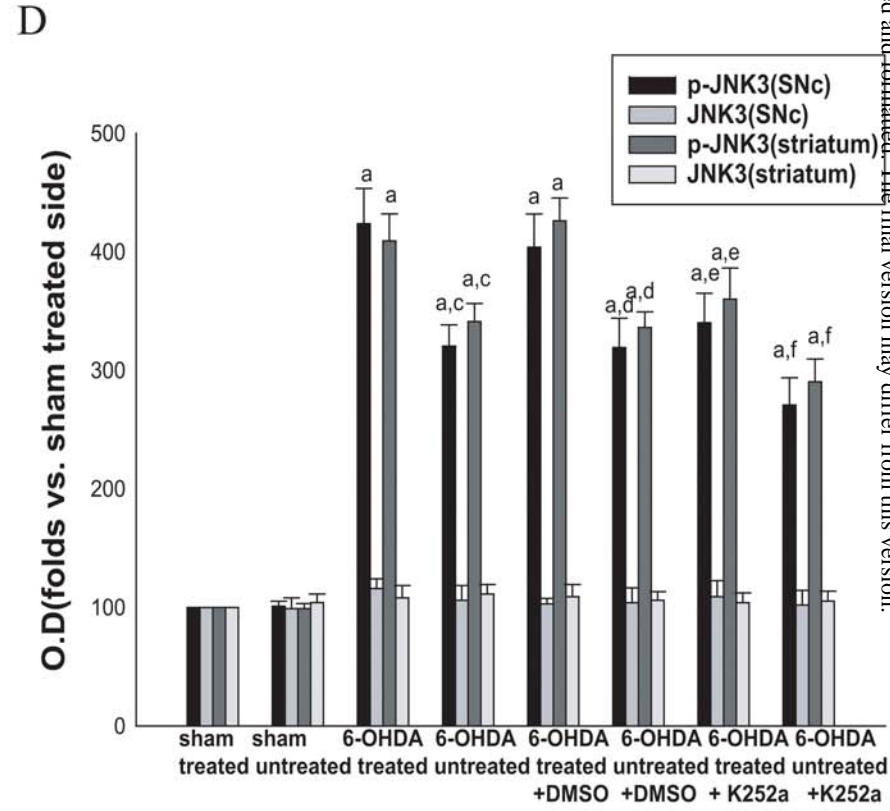
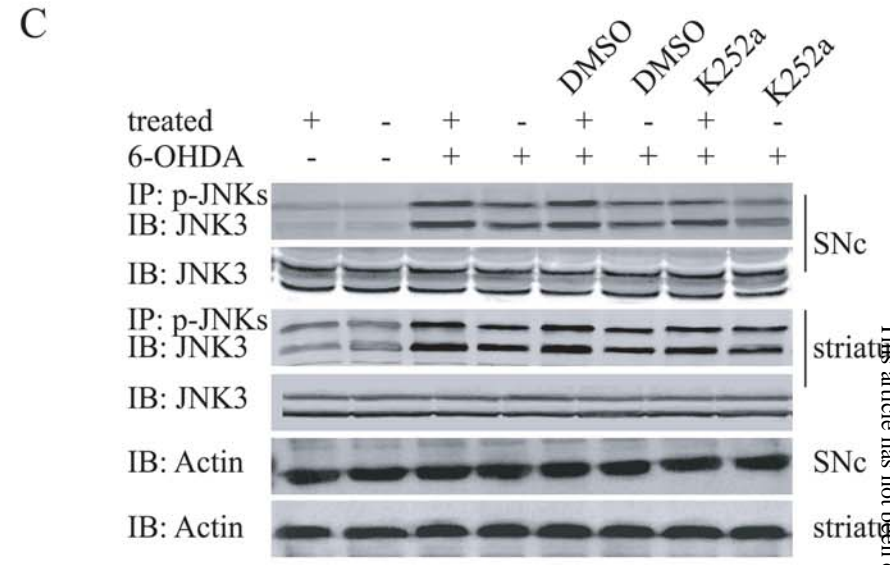
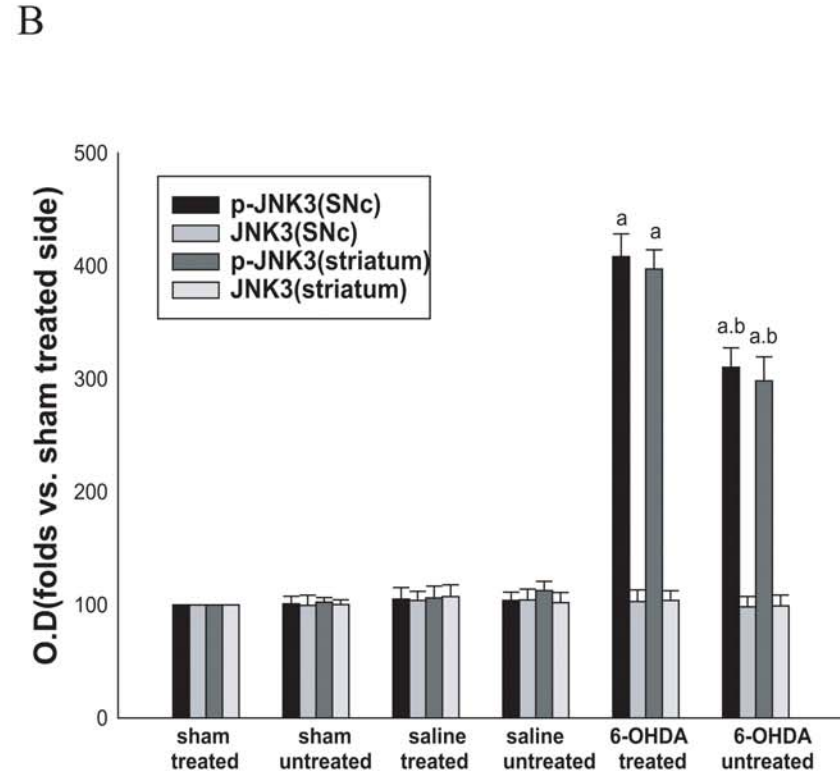
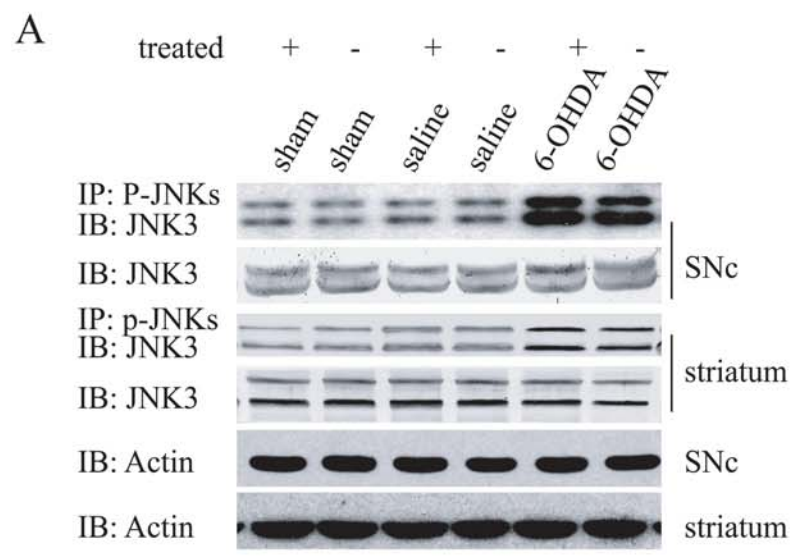


Fig. 3

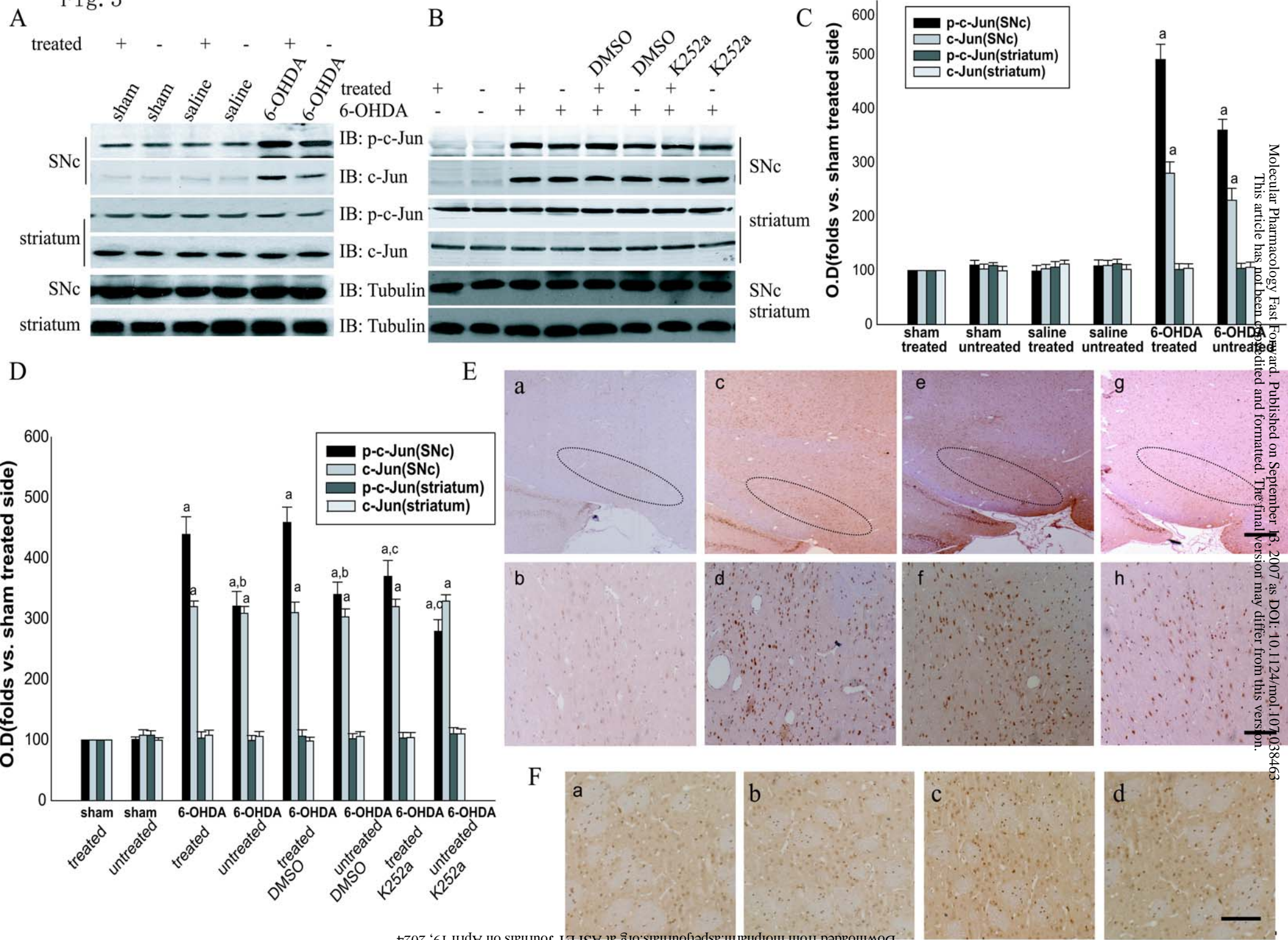


Fig. 4

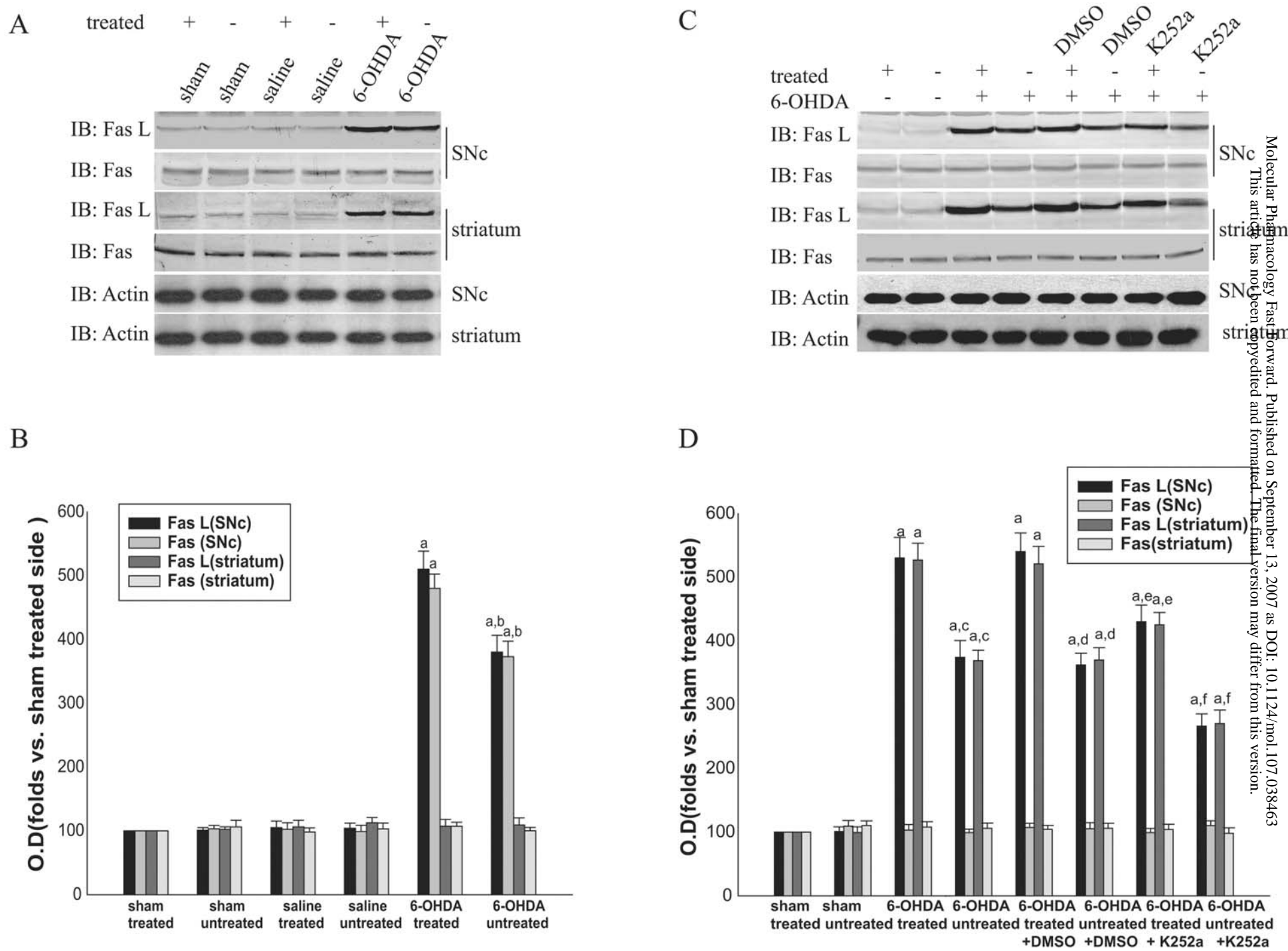


Fig. 5

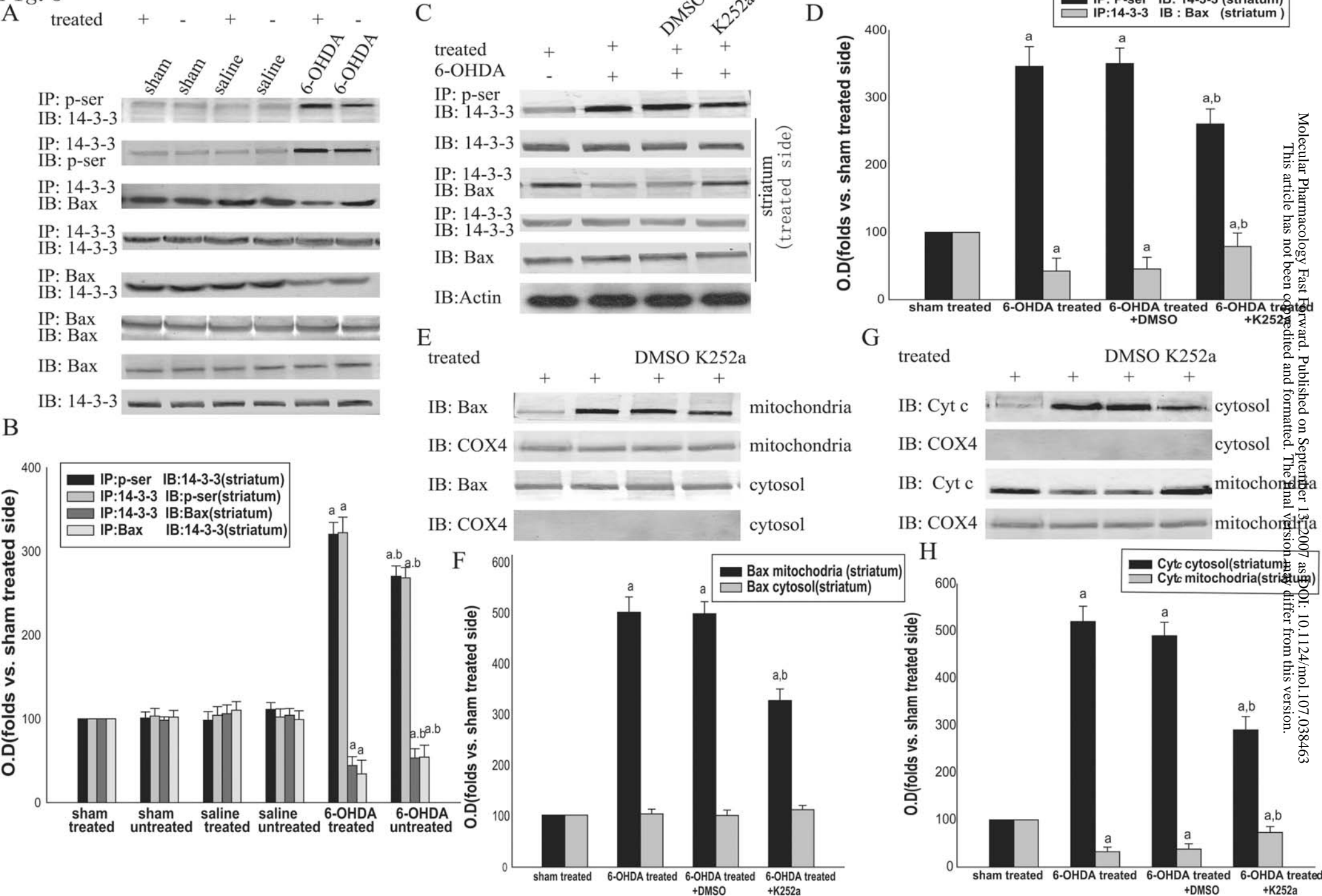


Fig. 6

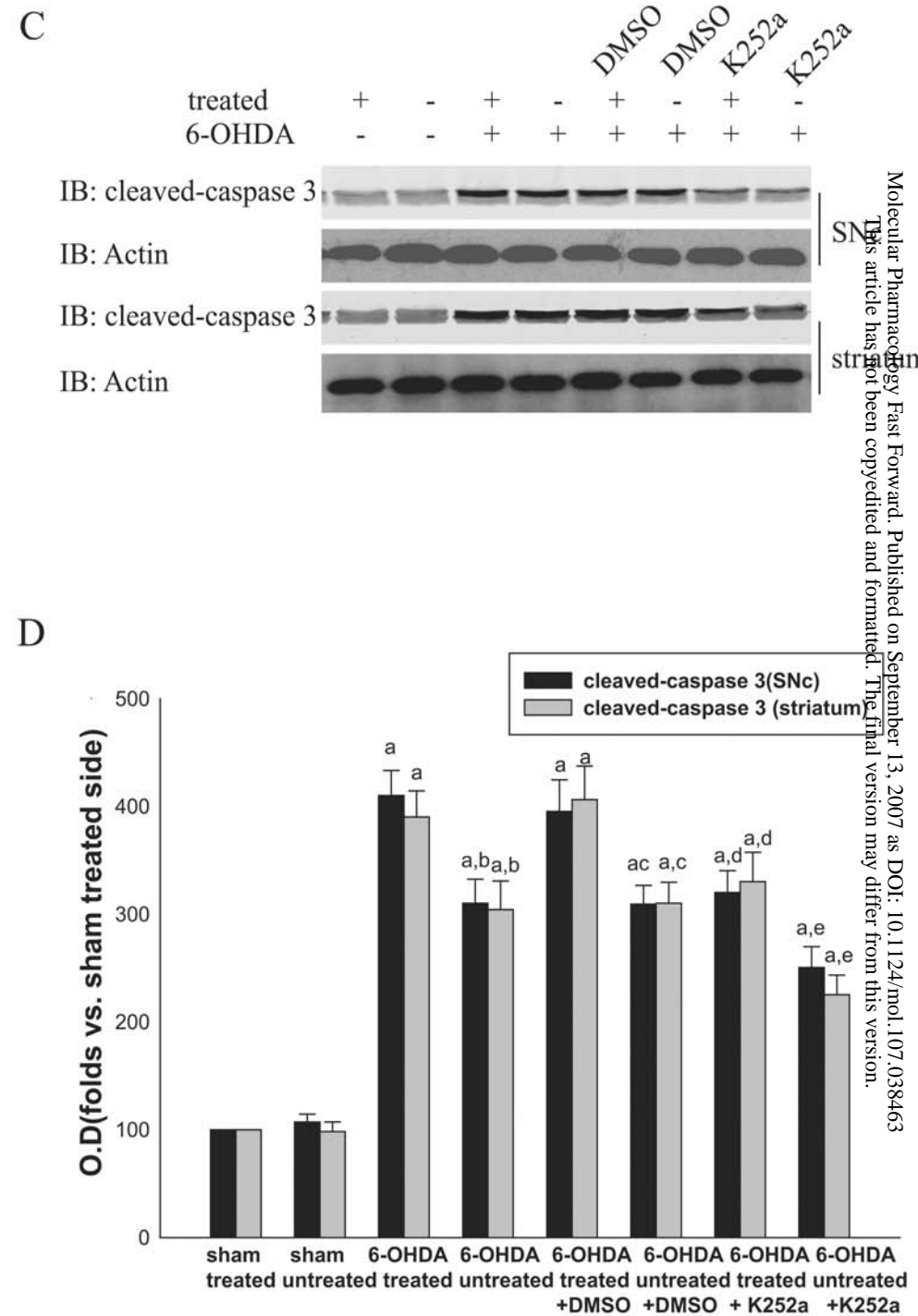
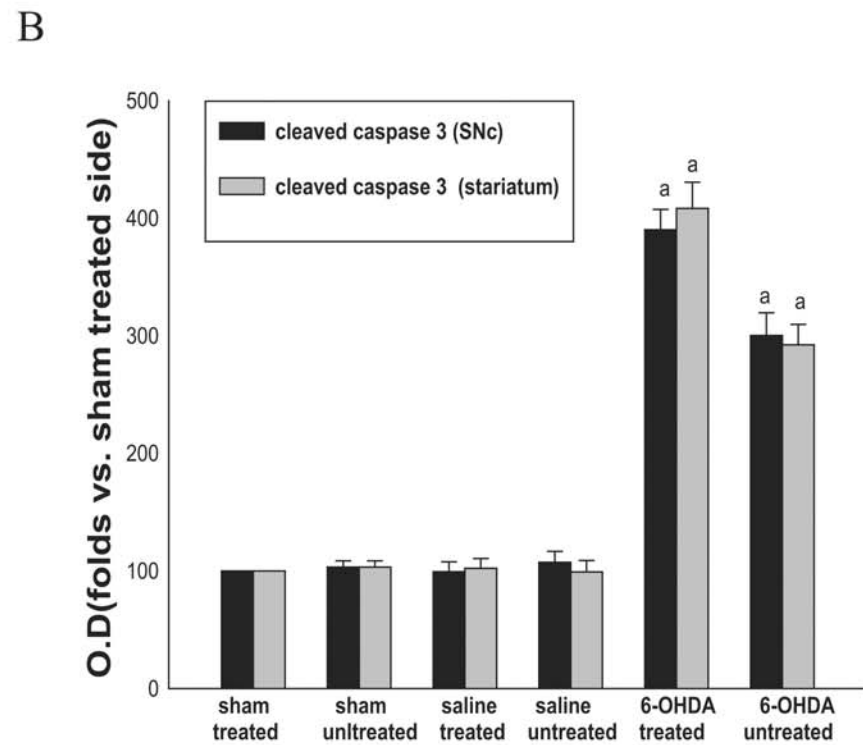
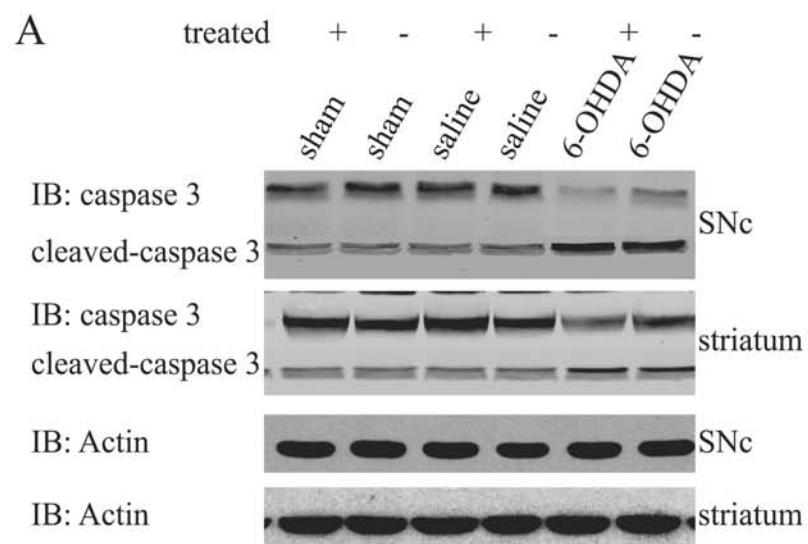


Fig. 7

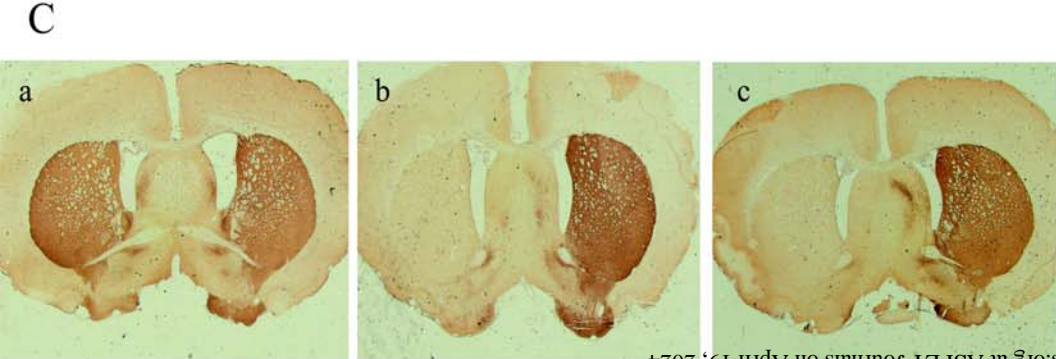
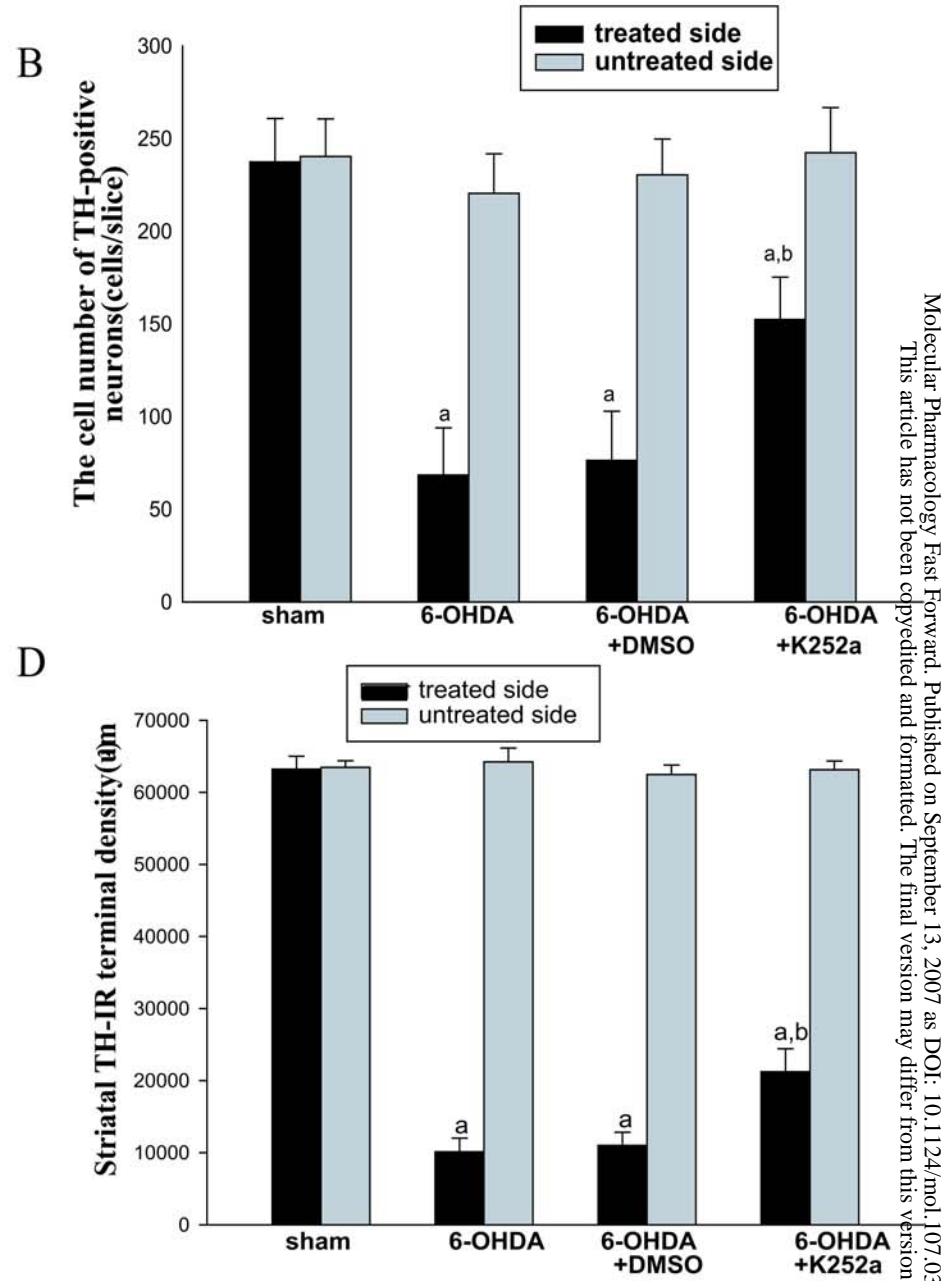
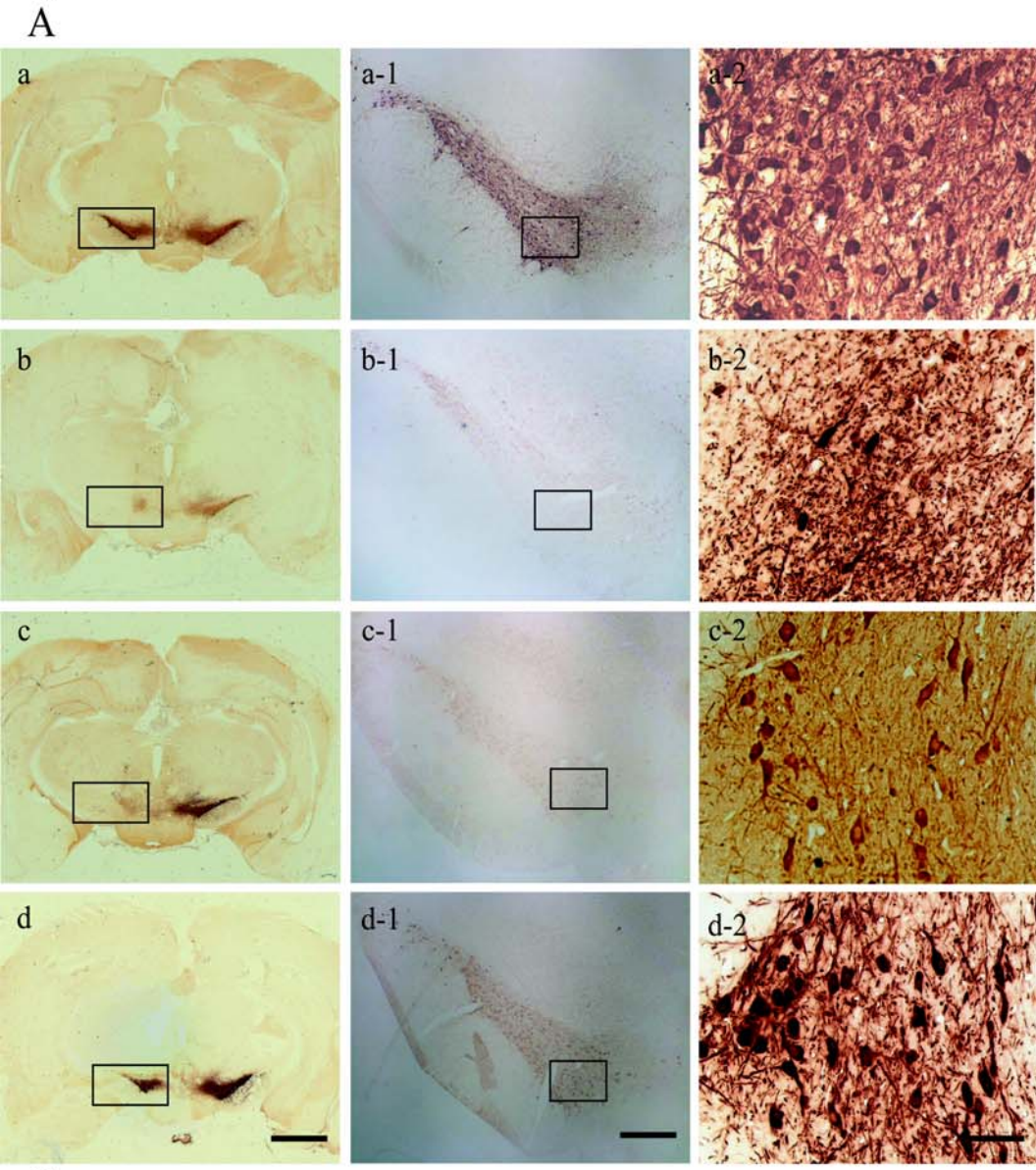


Fig. 8

